Formation and Coalescence Properties of Microbubbles

Scientific Note

M. D. BREDWELL, M. D. TELGENHOFF,
AND R. M. WORDEN*

*Department of Chemical Engineering,
Michigan State University, East Lansing, MI 48824*

Index Entries: Microbubble; aphron; foam; fermentation; mass transfer.

INTRODUCTION

Fermentations that involve a gaseous substrate are inherently rate-limited by mass transfer from the gaseous to the liquid phase. Aerobic and synthesis-gas fermentations are primary examples of such mass-transfer-limited fermentations. The traditional approach to enhance gas-to-liquid mass transfer is to increase the impeller rate, thereby increasing the interfacial area available for mass transfer. However, this approach results in a dramatic increase in power consumption, especially for large-scale systems, because power consumption is proportional to the impeller rate to the third power and the impeller diameter to the fifth power (*1*). Microbubble dispersions offer an alternative, providing high interfacial area with the potential for low power input. In aerobic fermentations with yeast, the transport of oxygen from a gas to a liquid, reported in terms of k_1a, was found to be greater by an order of magnitude using microbubble sparging oven conventional air sparging (2).

Microbubbles are surfactant-stabilized, spherical bubbles with diameters on the order of 100 μm. By comparison, gas bubbles found in conventional sparging units range from 3-5 mm (2). The surfactant layer surrounding the microbubble generates a diffuse electric double layer that

*Author to whom all correspondence and reprint requests should be addressed.

acts to repel other bubbles and prevent coalescence (3). A microbubble dispersion exhibits colloidal properties and is stable enough to be pumped (4).

This article examines the effects of surfactant type and concentration on microbubble formation, drainage, and stability. Effects of salts on microbubbles dispersions are examined as well. This information is needed to evaluate the utility of microbubble dispersions for biotechnological applications.

METHODS

The microbubble dispersions were formed using a spinning-disk device first described by Sebba (5). This device employs a rapidly spinning disk (>4000 rpm) and baffles to generate a localized high-shear zone that breaks apart bubbles larger than about 100 μm. The unit consists of a 6-L fermentation vessel with the impeller replaced by a 5-cm diameter, stainless-steel disk. A motor mounted above the head plate rotates the shaft at speeds up to 9000 rpm.

Bubble-size distributions were performed with a Malvern Mastersizer (Malvern, Inc.) particle size analyzer, which uses a light-scattering technique. In the formation-rate experiments, the dispersion was considered fully formed when an equilibrium foam volume was obtained. Dispersions were formed at 7000 rpm. Experiments were done with three types of surfactant: nonionic Triton X-100 (Sigma Chemical Co., St. Louis, MO), anionic sodium dodecyl sulfate (SDS) (Sigma Chemical Co.), and cationic cetyl pyridinium chloride (CPC) (Sigma Chemical Co.). Salt (NaCl) was added to the microbubble generator (MBG) in runs with Triton to determine its effects on microbubble formation.

In the drainage and stability experiments, the microbubble dispersion was generated, poured into a 1-L graduated cylinder (74 cm in height at 1 L, 6 cm in diameter), and allowed to drain. The heights of the air–foam and foam–liquid interfaces were measured as a function of time. Runs with NaCl were done in a similar fashion.

RESULTS

Figure 1 shows a typical bubble-size distribution.The number-averaged bubble diameter was 107 μm for Triton X-100 at a concentration twice that of the CMC and a temperature of 25°C.

Figure 2 shows the equilibrium formation time for microbubble dispersions as function of surfactant type and dimensionless surfactant concentration (DSC), which is defined as the ratio of surfactant concentration to its critical micelle concentration. Figure 3 shows the effects of NaCl on

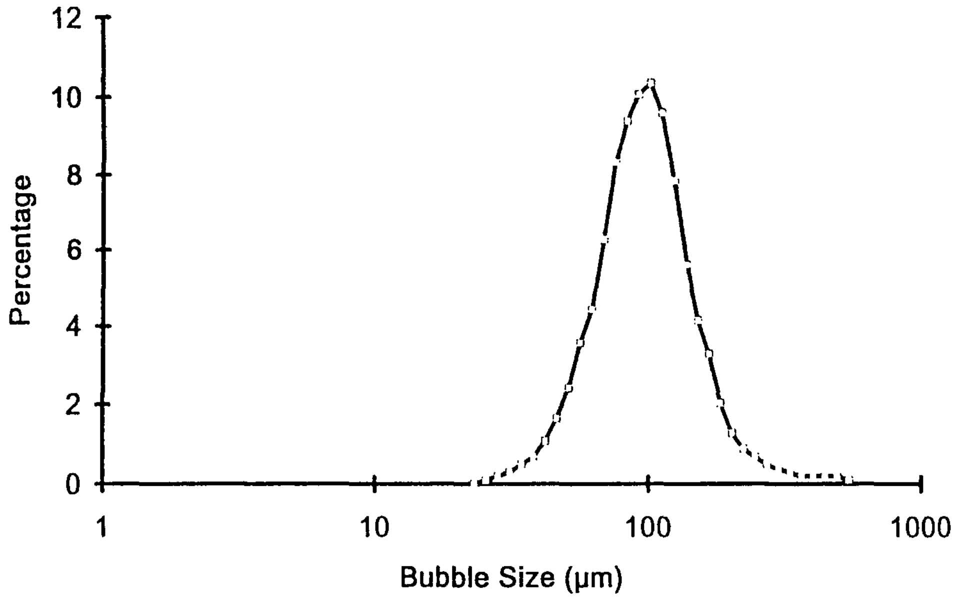

Fig. 1. Bubble size distribution.

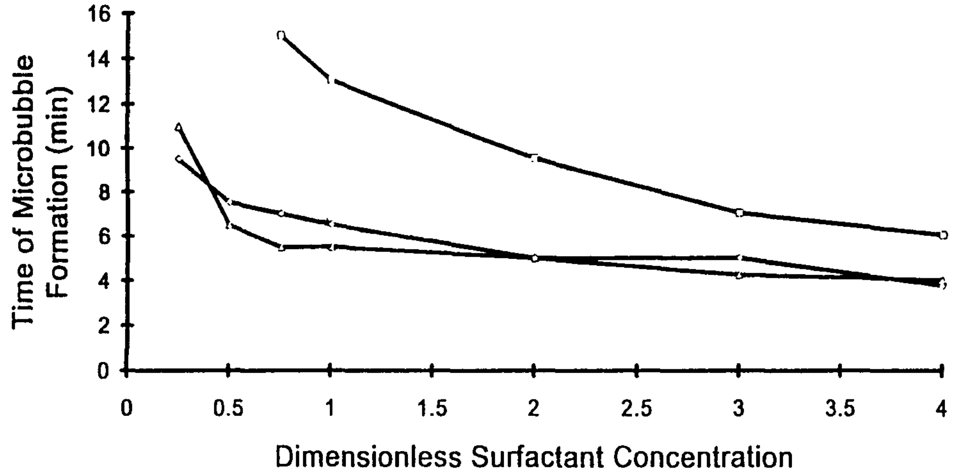

Fig. 2. Equilibrium formation time for microbubble foams as a function of surfactant concentration and surfactant type. □, Triton, nonionic; △, SDS, anionic; ◇, CPC, cationic.

the microbubble dispersion for Triton. Experiments were conducted at DSC values down to 0.25, but stable dispersions did not always form. If a stable dispersion did not form after 20 min, no data are shown for that concentration. A stable dispersion was taken to be indicated by a threefold volume expansion during foam formation.

Figure 4 shows a typical time-course for the drainage and stability experiments for an SDS foam with a DSC of 2. Figure 5 shows the effects

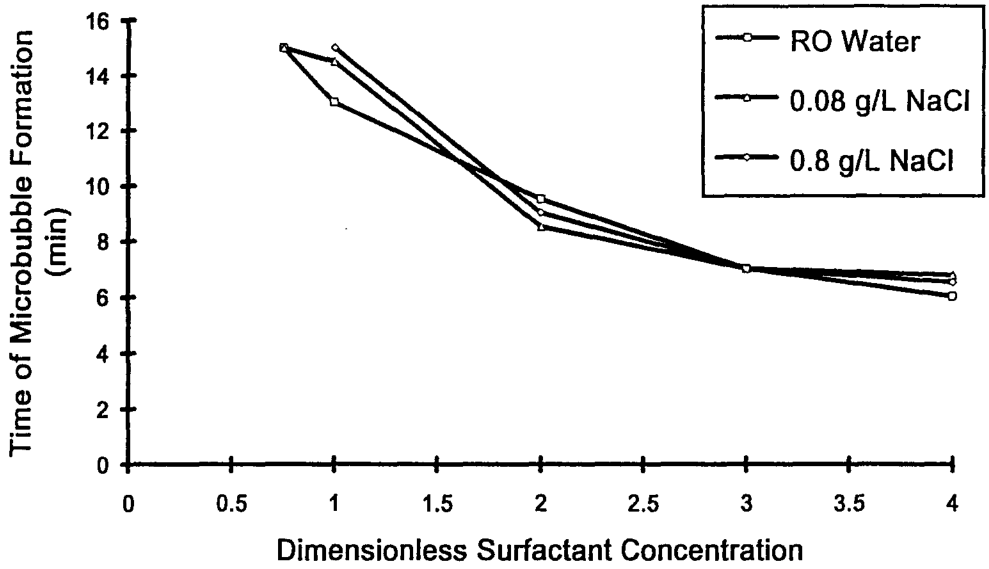

Fig. 3. Equilibrium formation time for microbubble foams as a function of surfactant and salt concentrations (for Triton). □, RO water;△ 0.08 g/L NaCl; 0.8 g/L NaCl.

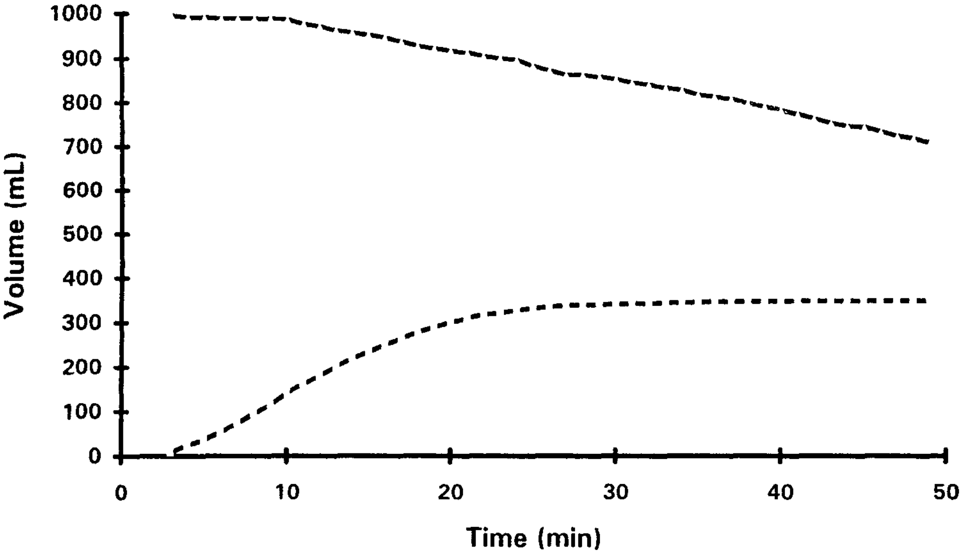

Fig. 4. Foam level (△) and foam-liquid interface level (□) as a function of time. The data plotted is for SDS with a DSC of 2.

of surfactant concentration on initial gas void fraction (ϵ_g^o). The value of ϵ_g^o was unaffected by NaCl in the range of 0–2.4 g/L for all surfactant concentrations tested (data not shown). Figure 6 shows foam stability, defined as the ratio of the volume of liquid drained after 4 min to the initial volume of foam, as a function of surfactant type and concentration.

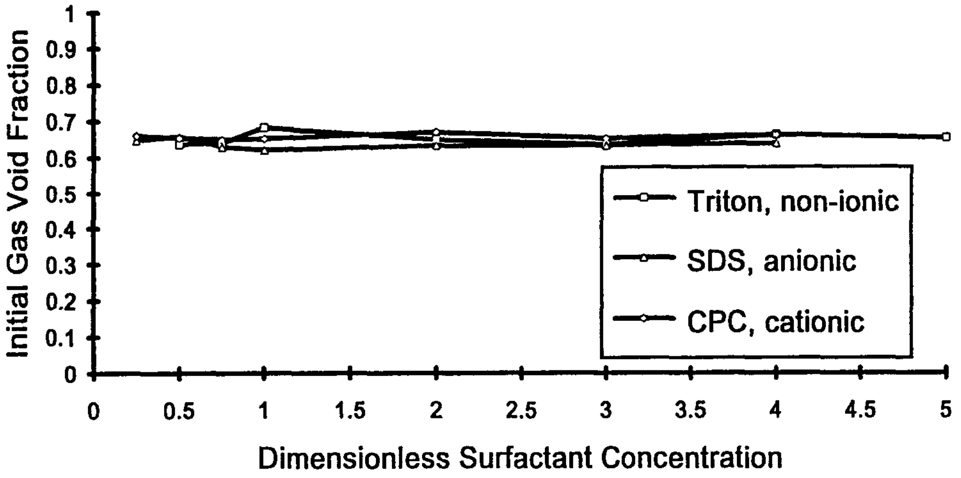

Fig. 5. Initial foam void fraction as a function of surfactant concentration and surfactant concentration and surfactant type. □, Triton, nonionic; △ SDS, anionic; ◇, CPC, cationic.

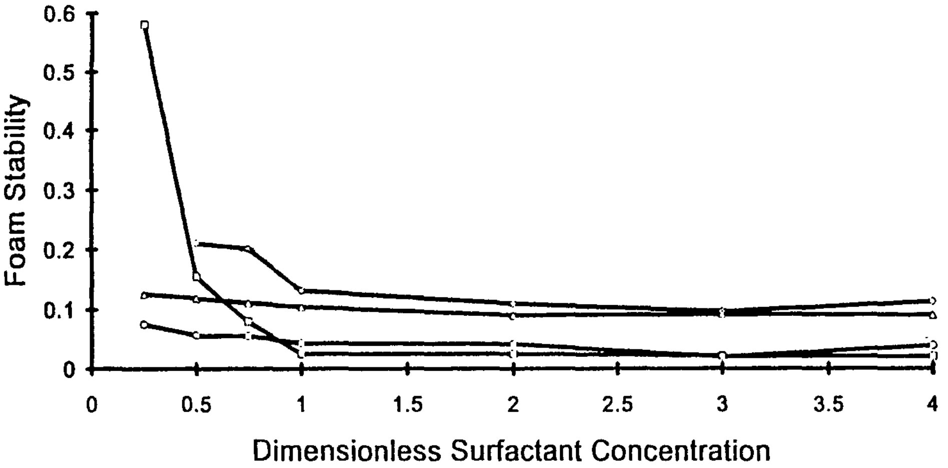

Fig. 6. Foam stability as a function of surfactant concentration and surfactant type. □, Triton, nonionic; ◇, Triton, with 0.08 g/L NaCl; △, CPC, cationic; ○, SDS, anionic.

DISCUSSION

The average bubble size measured by the Mastersizer is close to the values published in literature of 40–80 μm (*6*). Later modifications of the microbubble generator have allowed the generation of microbubbles in the 40–80 μm range (data not shown). The Mastersizer uses a light-scattering technique that gives accurate size distribution within seconds of injecting the sample. In contrast, microscope-based image-analysis methods are relatively slow and require many individual measurements to give statistically meaningful results.

The surfactant concentration is an important variable in the formation of stable dispersions. There is typically a double layer of surfactant around each microbubble (*3*); however, when the surfactant concentration is much below the CMC, stable microbubble dispersions do not form. In such cases, there is insufficient surfactant present to stabilize the large amount of interfacial area (*4*). Figure 2 indicates that as the surfactant concentration was increased above the CMC, the dispersion-formation decreased asymptotically to a value that is characteristic of the surfactant used. This trend is thought to be the result of saturation of the surfactant-adsorption capacity of the microbubbles. Further addition of surfactant has a negligible effect (*7*), because the additional surfactant molecules remain suspended in the fluid film surrounding the microbubbles. For ionic surfactants, such as CPC and SDS, the amount of surfactant necessary to achieve this asymptotic formation time was approximately the CMC. For the nonionic surfactant, the asymptote occurred at a higher concentration. This result may be owing in part to CMCs of ionic surfactants typically being higher than that of nonionic surfactants. In this study, the CMCs were 0.24 m*M* for Triton, 0.90 m*M* for CPC, and 8.27 m*M* for SDS. Ionic surfactants need to overcome the electrical repulsion of charged groups to form micelles (*8*). The number of surfactant molecules present at the CMC for ionic surfactants is therefore greater than that for nonionic surfactants. The addition of an electrolyte changes the CMC for ionic surfactants (*8*), presumably because charge shielding reduces intermolecular repulsion. However, salts have little effect on the CMC of nonionic surfactants (*3*). This trend is reflected in Fig. 3, in which dispersion-formation time was found to be independent of salt concentration.

Microbubble dispersions are an aggregate of spherical bubbles surrounded by a thin liquid film called the lamella. When the dispersion is first formed, the microbubbles are spherical, and the lamella is thick. Such dispersions are termed "wet" and have good stability (*3*). As the dispersion is allowed to drain, the liquid in the lamella drains into the plateau borders, regions where several bubbles meet. The liquid in the lamella drains in two different stages. Drainage occurs by gravity while the lamella are still thick and the microbubbles are still spherical. As the lamella thins, the microbubbles lose their spherical shape and begin to become polyhedral (*3*). At this stage, drainage of the dispersion is a result of surface-tension differences that depend on pressure differences throughout the lamella. The pressure differences arise from differences in the radius of curvature of the lamella. The greater the bubble size in the dispersion, the greater the drainage rate as a result of surface tensions differences (*7,8*). At some critical thickness of the lamella (50–100Å), the surrounding film will rupture (*8*).

When foam is poured into the graduated cylinder, buoyancy also contributes to foam settling. Microbubble dispersions will "cream" (i.e., faster rising bubbles will migrate to the surface). The time required for creaming depends on the rise velocity of the bubbles, which, according to Stokes law, is proportional to the bubble radius squared (*7*). The creaming process leads to a gradient in bubble size across the height of the column. Amiri and Woodburn (*9*) have shown that buoyancy effects result in a gradual increase in gas void fraction and bubble diameter from the bottom to the top in a column of microbubble dispersion.

Another factor contributing to the degradation of microbubble dispersions is "bubble ripening" (i.e., growth of larger bubbles at the expense of smaller ones). The difference in the interior pressures (ΔP) between two bubbles having radii R_1 and R_2, is given by the Laplace equation,

$$\Delta P = 2\sigma[(1/R_1) - (1/R_2)] \quad (1)$$

where σ is the surface tension. Because the pressure is greater inside smaller bubbles, there will be net transport of gas molecules through the liquid phase from smaller to larger bubbles. As the larger bubbles grow, they rise more rapidly and thus migrate to the top of the foam column.

The initial gas void fraction, ϵ_g^o, is a measure of the amount of gas initially trapped in the microbubble dispersion. Figure 5 shows ϵ_g^o to be independent of surfactant type and concentration, and approximately constant. The value of ϵ_g^o between 0.65 and 0.70, approaches 0.741, the tightest packing arrangement for monosized spheres in a face-centered cubic cell (*9,11*). For the nonionic surfactant, ϵ_g^o did not change with the addition of sodium chloride. The addition of salt also has little effect on the CMC for nonionic surfactants, as mentioned earlier (*3*).

Spherical bubble foams (also known as early or wet foams) are very stable, and will break only when the bubbles rise to the surface under the influence of gravity. As the foam begins to cream and drain, the bubbles grow larger and change their shape from spherical to polyhedral. Polyhedral bubbles can achieve a tighter packing; thus, the gas void fraction increases with not only height along the column, but also with time. Polyhedral foams (also known as late or dry foams) are much less stable. The lamellae of these foams thin as they drain and break when they can no longer resist the upward movement of the less dense gas trapped in the cells. The gas void fraction at which foams typically burst is 0.89 (*10*). Foam stability depends primarily on two factors: the rate of drainage of liquid from the lamella and strength of the film that encapsulates each bubble (*3*). At concentrations below the CMC, foam stability was found to increase with increasing surfactant concentration. At concentrations above the CMC, foam stability did not change appreciably with surfactant concentration. A possible explanation for this observation is that as the concentration of surfactant in the liquid phase increased, the density of surfactant adsorbed on the interface also increased until saturation was reached.

For successful use in fermentations, the surfactant should not inhibit cellular metabolism. In general, nonionic surfactants do not inactivate or denature enzymes and proteins (*12*). However, both anionic and cationic surfactants are prone to bind proteins. The charged groups of ionic surfactants form relatively strong ionic bonds with charged groups on the proteins. Nonionic surfactants, lacking the charged groups, bind through much weaker hydrophobic interactions with the protein chain (*12*). Nonionic surfactants would thus be expected to have the least influence on cellular metabolism in fermentation. However, ionic surfactants could be used if the concentration of the surfactant is kept below inhibitory levels. The use of mixed ionic/nonionic surfactant systems is another possibility (*4*).

CONCLUSIONS

The size distribution of microbubble dispersions can be rapidly measured using a light-scattering method. The number-averaged diameter for the microbubbles used in this study was 107 μm. Formation times of microbubble dispersions decreased with increasing surfactant concentration to an asymptotic value that varied with surfactant type. This asymptotic value was usually achieved at surfactant concentations around the CMC. Foam stability increased asymptotically with surfactant concentration to a constant value near the CMC.

Microbubble foams were found to have a constant initial gas void fraction that was independent of surfactant concentration and type. The experimental ϵ_g^0 value of 0.66 approaches the theoretical packing limit for monosized spheres. Salt concentrations from 0 to 2.4 g/L have virtually no effect on either the void fraction or the formation time for the nonionic surfactant.

ACKNOWLEDGMENTS

This material is based on work supported by the National Science Foundation under grant #BCS 92 20396, and fellowship support for M. D. Bredwell was provided from the NIH Biotechnology Training Program Grant and the Biotechnology Research Center at Michigan State University.

REFERENCES

1. McCabe, W. L., Smith, J. C., and Harriott, P. (1985), *Unit Operations of Chemical Engineering*, 4th ed., McGraw Hill, New York.
2. Kaster, J. A., Michelsen, D. L, and Velander, W. H. (1990), *Appl. Biochem. and Biotechnol.* **24/25**, 469-484.
3. Sebba, F. (1987), *Foams and Biliquid Foams—Aphrons*, Wiley, New York, pp. 47-78.

4. Longe, T. A. (1989), Colloidal Gas Aphrons: Generation, Flow Characterization and Application in Soil and Groundwater Decontamination, PhD. dissertation, Virginia Polytechnic Institute and State University.
5. Sebba, F. (1985), *Chem. and Ind.*, Feb. 4, 91,92.
6. Michelsen, D. L. and Lofti, M. (1991), *Biological Processes: Innovative Hazardous Waste Treatment Technology Series,* vol. 3, Technomic, Lancaster, PA, pp. 131–142.
7. Vold, R. D. and Vold, M. J. (1983), *Colloid and Interface Chemistry,* Addison-Wesley, Reading, MA, pp. 395–437.
8. Rosen, M. J. (1989), *Surfactant and Interfacial Phenomena,* 2nd ed., Wiley, New York.
9. Amiri, M. C. and Woodburn, E. T. (1990), *Trans IChemE* **68-A,** 154–160.
10. Weaire, D., Pittet, N., Hutzler, S., and Pardal, D. (1993), *Phys. Rev. Lett.* **71-16,** 2670–2673.
11. Brown, T. L. and LeMay, H. E. (1981), *Chemistry: The Central Science,* 2nd ed., Prentice-Hall, Englewood Cliffs, NJ.
12. Schwuber, M. J. and Bartnik, F. G. (1980), Interaction of anionic surfactants with proteins, enzymes, and membranes, in *Anionic Surfactants: Biochemistry, Toxicology, Dermatology,* Marcel Dekker, New York, pp. 1–49.